



Published in final edited form as:

J Neurol. 2011 March ; 258(3): 380–385. doi:10.1007/s00415-010-5762-6.

T1rho ($T_{1\rho}$) MR imaging in Alzheimer' disease and Parkinson's disease with and without dementia

Mohammad Haris,

Department of Radiology, Center for Magnetic Resonance and Optical Imaging (CMROI), University of Pennsylvania, B1 Stellar-Chance Laboratories, 422 Curie Boulevard, Philadelphia, PA 19104-6100, USA

Anup Singh,

Department of Radiology, Center for Magnetic Resonance and Optical Imaging (CMROI), University of Pennsylvania, B1 Stellar-Chance Laboratories, 422 Curie Boulevard, Philadelphia, PA 19104-6100, USA

Kejia Cai,

Department of Radiology, Center for Magnetic Resonance and Optical Imaging (CMROI), University of Pennsylvania, B1 Stellar-Chance Laboratories, 422 Curie Boulevard, Philadelphia, PA 19104-6100, USA

Christos Davatzikos,

SBIA, University of Pennsylvania, Philadelphia, PA, USA

John Q. Trojanowski,

Department of Pathology and Lab Medicine, University of Pennsylvania, Philadelphia, PA, USA

Elias R. Melhem,

Department of Radiology, University of Pennsylvania, Philadelphia, PA, USA

Christopher M. Clark, and

Department of Neurology, University of Pennsylvania, Philadelphia, PA, USA

Arijitt Borthakur

Department of Radiology, Center for Magnetic Resonance and Optical Imaging (CMROI), University of Pennsylvania, B1 Stellar-Chance Laboratories, 422 Curie Boulevard, Philadelphia, PA 19104-6100, USA

Abstract

In the current study, we aim to measure T1rho ($T_{1\rho}$) in the hippocampus in the brain of control, Alzheimer's disease (AD), Parkinson's disease (PD), and PD patients with dementia (PDD), and to determine efficacy of $T_{1\rho}$ in differentiating these cohorts. With informed consent, 53 AD patients, 62 PD patients, 11 PDD patients, and 46 age-matched controls underwent a standardized clinical assessment including mini-mental state examination (MMSE) and brain $T_{1\rho}$ MRI on a 1.5-T clinical-scanner. $T_{1\rho}$ maps were generated by fitting each pixel's intensity as a function of the spin-lock pulse duration. In control, AD, PD and PDD, mean \pm SE $T_{1\rho}$ values in the right

hippocampus (RH) were 92.15 ± 2.00 , 99.65 ± 1.98 , 85.68 ± 1.87 , 102.47 ± 4.66 ms while in the left hippocampus (LH) these values were 90.16 ± 1.82 , 99.53 ± 1.91 , 84.33 ± 2.03 , 95.33 ± 4.64 ms. Significant difference for both RH and LH $T_{1\rho}$ across the groups ($p < 0.001$) was observed. Both RH and LH $T_{1\rho}$ were significantly increased in AD compared to control ($p = 0.034$, $p = 0.001$) and PD ($p < 0.001$, $p < 0.001$). In control, both RH and LH $T_{1\rho}$ values were significantly increased compared to PD ($p = 0.031$, $p = 0.027$) while compared to PDD only the RH $T_{1\rho}$ value was significantly decreased ($p = 0.043$). Both RH and LH $T_{1\rho}$ values in PD were significantly lower than PDD ($p = 0.004$, $p = 0.032$). No significant correlation between the $T_{1\rho}$ and age as well as between $T_{1\rho}$ and MMSE scores was observed. The serial measurement of $T_{1\rho}$ in both AD and PD may provide the nature of disease progression and may contribute to their early diagnosis.

Keywords

T1rho MRI; Hippocampus; Alzheimer's disease; Parkinson disease; Parkinson disease with dementia

Introduction

Alzheimer's disease (AD) accounts for 50–60% of cases of dementia in the elderly [21]. Parkinson's disease (PD) is associated with the loss of dopaminergic neurons in the substantia nigra. Dementia is common and affects approximately 40% of PD patients during the course of the disease, the risk for the development of dementia in PD being six times higher than in non-PD age-matched controls [23].

Early and accurate diagnosis of both AD and PD are crucial for the patient's treatment. However, the diagnosis of both diseases is difficult in elderly patients because some of the key symptoms also may be manifestations of normal aging in both cases. Structural neuroimaging with MRI has the potential in the early diagnosis of both AD and PD [22, 28]. It has been shown that both AD and PD individuals showed high medial temporal lobe (MTL) atrophy compared to controls [29]. However, the contribution from normal age-related atrophy cannot easily be ruled out. Different neuroimaging studies have been proposed in the last few years to better characterize different structural or functional patterns that distinguish PD and PD patients with dementia (PDD) [6, 13]. A non-significant difference for MTL atrophy (MTA) between PD and PDD has been shown earlier [29].

Voxel based morphometry (VBM) has been used to measure the changes in brain volume in different neurodegenerative diseases [6, 13, 26]. However, VBM is not without its limitations. Spatial normalization is used to map each image to a template image in standard space, which has the potential to introduce errors since changes in brain volume are only on the order of a few percent. Although VBM detects atrophy of the hippocampus, these results may be insensitive to the detection of subtle changes/atrophy in areas of high variance, especially in small structures such as the hippocampus, resulting in a high variability among the elderly and diseased groups.

Functional imaging studies, such as single photon emission computed tomography (SPECT), positron emission tomography (PET), magnetic resonance spectroscopy, and diffusion tensor

imaging have been proposed in studying AD, PD and PDD [8, 11, 12, 15–17, 27]. It has been demonstrated that SPECT may not be a useful tool in the clinical differential diagnosis among PD, PDD and lewy body dementia and poor signal-to-noise ratios of the MRI techniques ultimately limits their sensitivity and reproducibility.

We have previously demonstrated that an alternate MRI contrast mechanism, $T_{1\rho}$ (T1rho), which is the spin lattice relaxation time constant in the rotating frame, can distinguish between AD and age-matched controls [5, 10]. In biological tissues, $T_{1\rho}$ relaxation may have contributions from several interactions. The interactions that are studied using this methodology can be broadly categorized into (1) dipole-dipole, (2) chemical exchange and (3) scalar-coupling processes [4]. Depending upon the tissue type, more than one mechanism may be operative simultaneously but with different relative contributions. In biological tissues, frequency dependence of relaxation rates or relaxation dispersion may arise from (1) rotational motion of a fraction of water bound to proteins, (2) exchange of protons on macromolecules with bulk water and (3) the non-averaged residual dipolar interaction of spin associated with oriented macromolecules in the tissue. $T_{1\rho}$ MRI has the capability to probe protein content in various tissues [14] and has been utilized to delineate brain tumors, characterize breast cancer tissue, and monitor the level of cartilage degeneration [1, 24, 25].

The aim of the current study was to measure $T_{1\rho}$ in the hippocampus in the brain of control, AD, PD, and PDD patients, and to determine whether $T_{1\rho}$ values can be used in differentiating these cohorts.

Materials and methods

Patient selection

The Institutional Review Board of University of Pennsylvania approved the study protocols. In the current study, we included 53 AD patients (mean age \pm SD = 77.5 \pm 8.1 years), 62 PD patients (mean age \pm SD = 70.5 \pm 6.1 years) without dementia, 11 PDD patients (mean age \pm SD = 76.2 \pm 3.7 years), and 46 age-matched controls (mean age \pm SD = 71.2 \pm 9.8 years).

All patients underwent a standardized clinical assessment including medical history, physical and neurological examination, psychometric evaluation, and brain MRI. The mini-mental state examination (MMSE) was used as a measure of general cognitive function. Diagnoses were made in conference by a team made up of a neurologist, neuropsychologists, a neurophysiologist and a psychiatrist. Diagnoses was made according the National Institute of Neurological and Communicative Diseases and Stroke/Alzheimer's Disease and Related Disorders Association criteria (NINCDS–ADRDA) for probable AD [19], the consensus criteria for PDD [18] and the UK Parkinson's Disease Society Brain Bank criteria for Parkinson's disease [9]. All Alzheimer's disease subjects met the criteria for probable Alzheimer's disease, while all Parkinson's disease and PDD subjects met the clinical diagnostic criteria for Parkinson's disease. Patients were excluded if they had a history of significant electrocardiographic (ECG) abnormalities; hematologic disorders; active malignancy within 5 years; or clinically important depressive, neuropsychiatric, cerebrovascular, or respiratory disease. Patients with hemorrhagic lesions as detected on MRI were also excluded from the study. The control group consisted of patients who

presented to our memory clinic with subjective complaints, and underwent exactly the same diagnostic work-up as the AD and PD patients.

MRI protocol

Written informed consent was obtained from each patient before they underwent MRI. All volunteers underwent MRI on a 1.5-T Siemens Sonata clinical scanner using the vendor-supplied 8-channel head coil. For $T_{1\rho}$ MRI, a fluid-attenuated $T_{1\rho}$ pre-encoded Turbo Spin-Echo pulse sequence was used [2]. The imaging parameters were: TR/TE = 2,000/12 ms, TSL (duration of spin lock pulse) = 10, 20, 30, 40 ms, with a spin lock B1 amplitude of 500 Hz, slice thickness = 2 mm, FOV = 22 cm, matrix size = 256×128 , bandwidth = 130 Hz/pixel, echo train length = 4 for a total imaging time of 6 min for four images. The inversion time (TI) was fixed at 860 ms to null the signal of CSF, removing the CSF contribution to $T_{1\rho}$ values. An oblique coronal $T_{1\rho}$ -weighted image of a slice perpendicular to the anterior/posterior commissure (AC/PC) plane was obtained. The slice was chosen to include the head of the hippocampus. Immediately after $T_{1\rho}$ MRI, the entire volume of each subject's brain was imaged for image segmentation using a T_1 -weighted 3D volumetric MPRAGE pulse sequence with 124 continuous slices in the coronal plane. The parameters were TR/TE = 3,000 ms/3.5 ms, slice thickness = 1.2 mm, FOV of 24 cm and 192 phase encode steps, and flip angle = 8° for a total imaging time of 10 min.

Data processing

The images were transferred to a G4 PowerBook computer (Apple Corp., Cupertino, CA, USA) and images were processed in the IDL programming language (RSI Cor., Boulder, CO, USA). The signal expression for the $T_{1\rho}$ -weighted MRI is given by the Eq. 1, 2.

$$M(\text{TSL}) = M_0 e^{-\text{TSL}/T_{1\rho}} \quad (1)$$

where M_0 is the thermal equilibrium magnetization.

The $T_{1\rho}$ relaxation time constant is dependent on the amplitude of the spin lock (SL) field, which is reported as a frequency, and typically ranges from zero to a few kilohertz. Equation 1 was linearized and then used to generate $T_{1\rho}$ maps by fitting each pixel's intensity as a function of TSL time using linear regression. $T_{1\rho}$ was calculated as $-1/\text{slope}$ of the straight-line fit. $T_{1\rho}$ of pixels that fitted poorly ($R^2 < 0.95$) were set to zero to remove background and noisy pixels.

Segmentation and automating reporting

The volumetric MPRAGE images were used to automatically report $T_{1\rho}$ values from the hippocampus by a custom written software described before ([5] Neuroimage). Briefly, the volumetric MPRAGE images were used to segment the brain into 92 anatomical structures [5] incorporating all major cortical and sub-cortical regions and coregistered with a standardized template [7]. The template's labels are then transformed to individual scans by applying the elastic transformation that was found to co-register with the respective $T_{1\rho}$ images. A program written in Matlab was used to automatically record $T_{1\rho}$ values from the

right hippocampus (RH) and left hippocampus (LH) onto an excel spreadsheet. The co-registration and the hippocampus segmentation were performed in the presence of an experienced neuroradiologist.

Statistical analyses

Descriptive statistics were performed to calculate the mean value of $T_{1\rho}$ in the RH and LH for different cohorts (control, AD, PD and PDD). Kruskal-Wallis ANOVA was performed followed by post hoc Mann-Whitney U test to compare the $T_{1\rho}$ values among the different cohorts (control, AD, PD and PDD). The Student's t test was performed between RH and LH $T_{1\rho}$ values for each cohort. Pearson correlations between $T_{1\rho}$ values versus age and between $T_{1\rho}$ versus MMSE score were performed separately for each cohort. A p value of less than 0.05 was considered to be statistically significant. All the statistical computations were performed using the Statistical Package for Social Sciences (SPSS) version 16.0 (SPSS Inc., Chicago, USA).

Results

The mean MMSE score in control, AD, PD and PDD were 29.1 ± 5.8 , 19.53 ± 5.8 , 27.4 ± 3.7 , 21.9 ± 3.8 , respectively. The average RH and LH $T_{1\rho}$ values in the brain of control, AD, PD and PDD are reported in Table 1. Kruskal-Wallis ANOVA showed significant difference for both RH and LH $T_{1\rho}$ across the four groups ($p < 0.001$). The Mann-Whitney test showed that both RH and LH $T_{1\rho}$ values were significantly increased in AD compared to control ($p = 0.034$, $p = 0.001$) and PD ($p < 0.001$, $p < 0.001$) while no significant difference was observed on comparing to PDD ($p = 0.539$, $p = 0.471$). In PD, both the RH and LH $T_{1\rho}$ values were significantly decreased relative to controls ($p = 0.031$, $p = 0.027$) and PDD ($p = 0.004$, $p = 0.032$). Only the RH $T_{1\rho}$ value was significantly decreased ($p = 0.043$) in controls compared to PDD.

In AD, the LH $T_{1\rho}$ value was 10% greater than control, 18% greater than PD and 4% greater than PDD while the RH $T_{1\rho}$ was 8% greater than control, 16% greater than PD and 3% less than PDD. In control, the LH $T_{1\rho}$ was 7% greater than PD and 6% less than PDD while the RH $T_{1\rho}$ was 7% greater than PD and 10% less than PDD. In PDD the LH $T_{1\rho}$ was 13% greater than PD while the RH $T_{1\rho}$ was 20% greater than PD.

In all the cohorts the RH $T_{1\rho}$ value was higher than the LH $T_{1\rho}$ value. In none of the cohorts did this difference reach to the statistically significant level. In control, AD, PD and PDD the RH $T_{1\rho}$ was 2, 0.1, 2, and 8% greater than LH $T_{1\rho}$.

Figure 1 shows $T_{1\rho}$ maps overlaid on fluid-attenuated $T_{1\rho}$ MR images. Pixels with higher $T_{1\rho}$ value in hippocampus in the brain of AD and PDD individuals are apparent from $T_{1\rho}$ maps (Fig. 1). Figure 2 represents box and whisker plots of $T_{1\rho}$ in different cohorts. In the right hippocampus two outliers are found in the case of AD cohort.

We analyzed the gender related changes in $T_{1\rho}$ in different cohorts (control, AD, and PD). In all cohorts, both the right and left hippocampus $T_{1\rho}$ values were higher in female compared to the male. However, in none of the cohorts $T_{1\rho}$ difference reach to the statistical significant

level. No significant correlation between the $T_{1\rho}$ and age as well as between $T_{1\rho}$ and MMSE scores was observed.

Discussion

In the current study, we found significantly increased $T_{1\rho}$ in the hippocampus in the brain of AD and PDD compared to control and PD. The PD individuals showed significantly decreased $T_{1\rho}$ value compared to controls. Also, no significant difference between the RH $T_{1\rho}$ and LH $T_{1\rho}$ for any of the cohort was noted.

The feasibility of $T_{1\rho}$ in the detection of plaques burden in the mice model of AD has been already reported [3]. Recently, Borthakur et al. [5] have shown increased $T_{1\rho}$ in MTL of AD compared to controls. Further, Haris et al. [10] showed the significantly increased $T_{1\rho}$ in the hippocampus of the MCI and AD compared to controls. All these studies suggested that the presence of AD pathology may contribute to the molecular interactions such as exchanging protons from bulk water with protons associated with slowly tumbling macromolecules in the extracellular space resulting in an increased $T_{1\rho}$.

Earlier, increased $T_{1\rho}$ has been reported in substantia nigra in the brain of PD patients and suggested the possible role of neuronal loss in increased $T_{1\rho}$ [20]. However, in the current study, we found decreased hippocampus $T_{1\rho}$ in PD even compared to controls. Pathological studies of the brains of patients who died of Parkinson disease have demonstrated increased iron content in the substantia nigra. Because iron accumulation affects the MR signal, attempts have been made to monitor the changes in iron content in patients with Parkinson disease by using MR T_2 relaxometry. Here, we suggest that the decreased $T_{1\rho}$ in PD is probably due to proton spin dephasing from iron-induced local field inhomogeneities resulting from the increased iron content in the substantia nigra. No attempt was made to quantify iron content in the hippocampus in the brain of PD and PDD patients; however, such study could further help in understanding the $T_{1\rho}$ mechanism. The Vymazal et al. [30] have shown non-significantly decreased T_2 in the substantia nigra. In the current study, we found significantly decreased $T_{1\rho}$ in PD compared to controls suggestive of $T_{1\rho}$ is more sensitive than T_2 in detection of the pathological changes. No T_2 measurement was performed in the current study as the aim of this study was to define the $T_{1\rho}$ values in the different pathological conditions. However, $T_{1\rho}$ MRI has been previously used to measure $T_{1\rho}$ relaxation time in normal human brain, and showed higher range of values compared to T_2 .

Brain atrophy rate was significantly increased in PDD compared to PD and control, while no significant difference for brain atrophy was found between PD and control [6]. It has been also shown that in PDD, the degree of hippocampal atrophy may be similar to or even more severe than AD [13]. The number of AD changes has been shown to be higher in PDD patients compared to PD without dementia. Laakso et al. [13] reported that the absolute volume of the hippocampus in PDD was smaller than that of Alzheimer's disease patients, although not significantly so, while the coexistence of Alzheimer's disease pathology in the Parkinson's disease group could not be ruled out. The PDD and AD groups also did not differ in the distribution of the MMSE score, which reflect global cognitive function. We

suggest that the increased $T_{1\rho}$ in PDD may be associated with the increased atrophy and high AD related changes.

Our data suggest that bilateral hippocampus $T_{1\rho}$ changes in AD, PD and PDD compared to the control is consistent with the earlier findings which showed bilateral hippocampus volume loss in AD and PDD. No significant correlation was observed between $T_{1\rho}$ and age in all cohorts suggesting that the change in $T_{1\rho}$ is due to the underlying pathophysiology instead of any age related changes. Further, no significant correlation between MMSE score and $T_{1\rho}$ suggests that cognitive score may not enough sensitive to the tissue pathology.

In our study, as in many of the previous imaging studies, there was considerable overlap between patient groups. We believe this overlap is due to the large variation in the $T_{1\rho}$ values in PDD individuals as also depicted by the graphs. The variation in $T_{1\rho}$ in PDD groups might be due to the small sample size. We did not correlate $T_{1\rho}$ with the atrophy rate as well as hippocampus volume, which may be considered the limitation of the current study. Another potential limitation of our study is the reliance on clinical, rather than autopsy proven, diagnoses.

The two-dimensional $T_{1\rho}$ -weighted MRI pulse sequence was used for the measurement of $T_{1\rho}$ which is limited to a single-slice acquisition since the SL pulse cannot be made slice selective. We have already developed and implemented a three-dimensional $T_{1\rho}$ -weighted pulse sequence on a 1.5-T clinical scanner [31]. $T_{1\rho}$ values measured with this sequence agree with those obtained by a previously validated two-dimensional $T_{1\rho}$ imaging sequence [2]. Furthermore, the 3D images will allow for direct comparison of $T_{1\rho}$ values and brain atrophy rates in several regions of the brain such as the entire hippocampus and entorhinal cortex.

In conclusion, measurement of $T_{1\rho}$ in both AD and PD may contribute to their early diagnosis in the future. Further, measurement of hippocampus $T_{1\rho}$ may help with the early diagnosis of dementia in PD, something that now requires a further investigation by serially monitoring PD patients. In the future, it may important to investigate regional rates of $T_{1\rho}$ changes and the role of serial $T_{1\rho}$ MRI in the assessment of treatments for slowing disease progression.

Acknowledgments

This work was performed at a NIH supported resource center (NIH RR02305) and from a grant from the Pennsylvania State Tobacco Settlement.

References

1. Aronen HJ, Ramadan UA, Peltonen TK, Markkola AT, Tanttu JI, Jääskeläinen J, Häkkinen AM, Sepponen R. 3D spin-lock imaging of human gliomas. *Magn Reson Imaging*. 1999; 17:1001–1010. [PubMed: 10463651]
2. Borthakur A, Wheaton AJ, Gougoutas AJ, Akella SV, Regatte RR, Charagundla SR, Reddy R. In vivo measurement of T1rho dispersion in the human brain at 1.5 Tesla. *J Magn Reson Imaging*. 2004; 19:403–409. [PubMed: 15065163]

3. Borthakur A, Gur T, Wheaton AJ, Corbo M, Trojanowski JQ, Lee VM, Reddy R. In vivo measurement of plaque burden in a mouse model of Alzheimer's disease. *J Magn Reson Imaging*. 2006; 24:1011–1017. [PubMed: 17036339]
4. Borthakur A, Mellon E, Niyogi S, Witschey W, Kneeland JB, Reddy R. Sodium and T1rho MRI for molecular and diagnostic imaging of articular cartilage. *NMR Biomed*. 2006; 19:781–821. [PubMed: 17075961]
5. Borthakur A, Sochor M, Davatzikos C, Trojanowski JQ, Clark CM. T1rho MRI of Alzheimer's disease. *Neuroimage*. 2008; 41:1199–1205. [PubMed: 18479942]
6. Burton EJ, McKeith IG, Burn DJ, Williams ED, O'Brien JT. Cerebral atrophy in Parkinson's disease with and without dementia: a comparison with Alzheimer's disease, dementia with Lewy bodies and controls. *Brain*. 2004; 127:791–800. [PubMed: 14749292]
7. Davatzikos C, Fan Y, Wu X, Shen D, Resnick SM. Detection of prodromal Alzheimer's disease via pattern classification of magnetic resonance imaging. *Neurobiol Aging*. 2008; 29:514–523. [PubMed: 17174012]
8. Firbank MJ, Harrison RM, O'Brien JT. A comprehensive review of proton magnetic resonance spectroscopy studies in dementia and Parkinson's disease. *Dement Geriatr Cogn Disord*. 2002; 14:64–76. [PubMed: 12145453]
9. Gibb WRG, Lees AJ. The relevance of the Lewy body to the pathogenesis of idiopathic Parkinson's disease. *J Neurol Neurosurg Psychiatry*. 1988; 51:745–752. [PubMed: 2841426]
10. Haris M, McArdle E, Fenty M, Singh A, Davatzikos C, Trojanowski JQ, Melhem ER, Clark CM, Borthakur A. Early marker for Alzheimer's disease: hippocampus T1rho estimation. *J Magn Reson Imaging*. 2009; 29:1008–1012. [PubMed: 19388096]
11. Ito K, Nagano-Saito A, Kato T, Arahata Y, Nakamura A, Kawasumi Y, Hatano K, Abe Y, Yamada T, Kachi T, Brooks DJ. Striatal and extrastriatal dysfunction in Parkinson's disease with dementia: a 6-[18F]fluoro-L-dopa PET study. *Brain*. 2002; 125:1358–1365. [PubMed: 12023324]
12. Johnson KA, Holman BL, Mueller SP, Rosen TJ, English R, Nagel JS, Growdon JH. Single photon emission computed tomography in Alzheimer's disease. Abnormal iofetamine I 123 uptake reflects dementia severity. *Arch Neurol*. 1988; 45:392–396. [PubMed: 3258512]
13. Laakso MP, Partanen K, Riekkinen P, Lehtovirta M, Helkala EL, Hallikainen M, Hanninen T, Vainio P, Soininen H. Hippocampal volumes in Alzheimer's disease, Parkinson's disease with and without dementia, and in vascular dementia: an MRI study. *Neurology*. 1996; 46:678–681. [PubMed: 8618666]
14. Mäkelä HI, De Vita E, Gröhn OH, Kettunen MI, Kavcic M, Lythgoe M, Garwood M, Ordidge R, Kauppinen RA. B0 dependence of the on-resonance longitudinal relaxation time in the rotating frame (T1rho) in protein phantoms and rat brain in vivo. *Magn Reson Med*. 2004; 51:4–8. [PubMed: 14705038]
15. Matsui H, Uda F, Miyoshi T, Hara N, Tamura A, Oda M, Kubori T, Nishinaka K, Kameyama M. *N*-isopropyl-*p*-123I iodoamphetamine single photon emission computed tomography study of Parkinson's disease with dementia. *Intern Med*. 2005; 44:1046–1050. [PubMed: 16293914]
16. Matsui H, Nishinaka K, Oda M, Niikawa H, Kubori T, Uda F. Dementia in Parkinson's disease: diffusion tensor imaging. *Acta Neurol Scand*. 2007; 116:177–181. [PubMed: 17714331]
17. McGeer PL, Kamo H, Harrop R, Li DK, Tuokko H, McGeer EG, Adam MJ, Ammann W, Beattie BL, Calne DB, et al. Positron emission tomography in patients with clinically diagnosed Alzheimer's disease. *CMAJ*. 1986; 134:597–607. [PubMed: 3512063]
18. McKeith IG, Galasko D, Kosaka K, Perry EK, Dickson DW, Hansen LA, et al. Consensus guidelines for the clinical and pathologic diagnosis of dementia with Lewy bodies (DLB): report of the consortium on DLB international workshop. *Neurology*. 1996; 47:1113–1124. [PubMed: 8909416]
19. McKhann G, Drachman D, Folstein M, Katzman R, Price D, Stadlan EM. Clinical diagnosis of Alzheimer's disease: report of the NINCDS-ADRDA Work Group under the auspices of Department of health and human services task force on Alzheimer's Disease. *Neurology*. 1984; 34:939–944. [PubMed: 6610841]
20. Michaeli S, Liimatainen T, Rydeen CE, Kotz CM, Nixon JP, Hanson T, Tuite PJ. T(1rho) and T(2rho) MRI in the evaluation of Parkinson's disease. *J Neurol*. 2010 (Epub ahead of print).

21. Nussbaum RL, Ellis CE. Alzheimer's disease and Parkinson's disease. *N Engl J Med.* 2003; 348:1356–1364. [PubMed: 12672864]
22. O'Brien J, Barber B. Neuroimaging in dementia and depression. *Adv Psychiatr Treat.* 2000; 6:109–119.
23. Padovani A, Costanzi C, Gilberti N, Borroni B. Parkinson's disease and dementia. *Neurol Sci.* 2006; 1:S40–S43.
24. Regatte RR, Akella SV, Wheaton AJ, Lech G, Borthakur A, Kneeland JB, Reddy R. 3D-T1rho-relaxation mapping of articular cartilage: in vivo assessment of early degenerative changes in symptomatic osteoarthritic subjects. *Acad Radiol.* 2004; 11:741–749. [PubMed: 15217591]
25. Santyr GE. MR imaging of the breast imaging and tissue characterization without intravenous contrast. *Magn Reson Imaging Clin N Am.* 1994; 2:673–690. [PubMed: 7489316]
26. Senjem ML, Gunter JL, Shiung MM, Petersen RC, Jack CR Jr. Comparison of different methodological implementations of voxel-based morphometry in neurodegenerative disease. *Neuroimage.* 2005; 26:600–608. [PubMed: 15907317]
27. Stebbins GT, Murphy CM. Diffusion tensor imaging in Alzheimer's disease and mild cognitive impairment. *Behav Neurol.* 2009; 21:39–49. [PubMed: 19847044]
28. Summerfield C, Junqué C, Tolosa E, Salgado-Pineda P, Gómez-Ansón B, Martí MJ, Pastor P, Ramírez-Ruiz B, Mercader J. Structural brain changes in Parkinson disease with dementia: a voxel-based morphometry study. *Arch Neurol.* 2005; 62:281–285. [PubMed: 15710857]
29. Tam CW, Burton EJ, McKeith IG, Burn DJ, O'Brien JT. Temporal lobe atrophy on MRI in Parkinson disease with dementia: a comparison with Alzheimer disease and dementia with Lewy bodies. *Neurology.* 2005; 64:861–865. [PubMed: 15753423]
30. Vymazal J, Righini A, Brooks RA, Canesi M, Mariani C, Leonardi M, Pezzoli G. T1 and T2 in the brain of healthy subjects, patients with Parkinson disease, and patients with multiple system atrophy: relation to iron content. *Radiology.* 1999; 211:489–495. [PubMed: 10228533]
31. Witschey WR, Borthakur A, Elliott MA, Fenty M, Sochor MA, Wang C, Reddy R. T1rho-prepared balanced steady-state free precession for rapid 3D T1rho-weighted MRI. *J Magn Reson Imaging.* 2008; 28:744–754. [PubMed: 18777535]

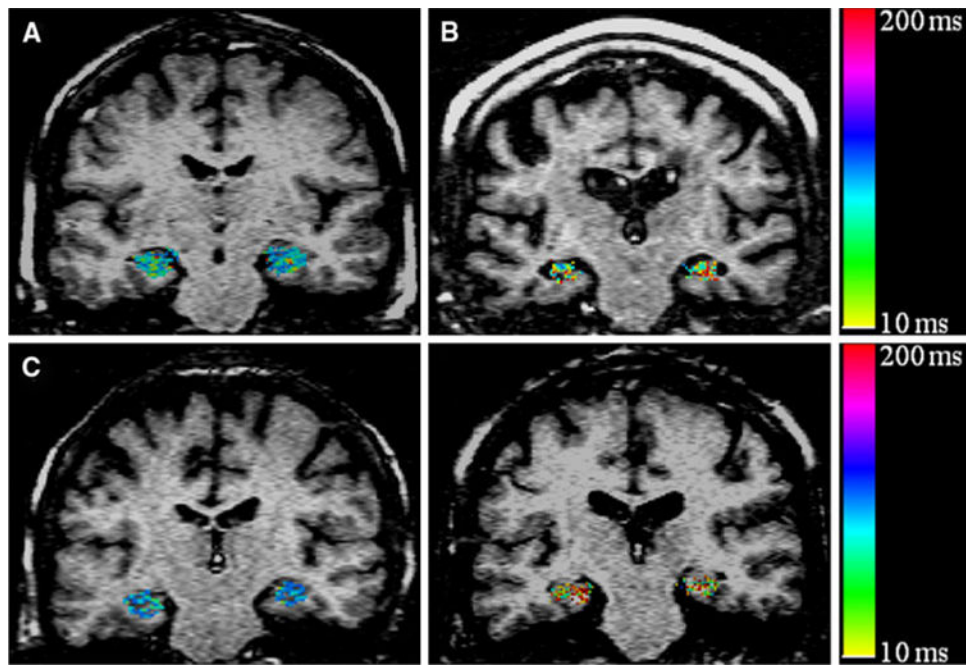


Fig. 1.

$T1\rho$ maps of the hippocampus region in the brain (in *color*) overlaid on fluid-attenuated $T1\rho$ MR image of control (77 Y male, **a**), AD (76 Y male, **b**), PD (71 Y female, **c**) and PDD patients (73 Y female, **d**). Pixels with higher $T1\rho$ (*red*) are more prominent in the hippocampus of AD and PDD patients. The PD patient shows decrease hippocampus $T1\rho$. No $T1\rho$ signal from CSF implies that the higher $T1\rho$ values are not due to fluid. *AD* Alzheimer's disease, *PD* Parkinson's disease, *PDD* Parkinson's disease with dementia

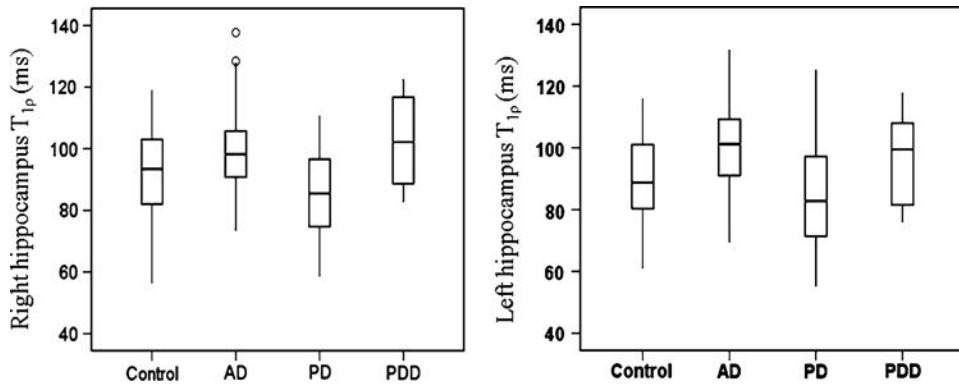


Fig. 2.

The *box* and *whisker plots* show the $T_{1\rho}$ value in right and left hippocampus in the brain of control, AD, PD and PDD cohorts. The right hippocampus $T_{1\rho}$ plot also shows the two outliers (*small circle*) in case of AD. *AD* Alzheimer's disease, *PD* Parkinson's disease, *PDD* Parkinson's disease with dementia

Table 1

The mean (\pm SD) $T_{1\rho}$ value in hippocampus in the brain of the different cohorts

Group	Hippocampus $T_{1\rho}$	
	Right	Left
Control	92.15 \pm 2.00	90.16 \pm 1.82
AD	99.65 \pm 1.98	99.53 \pm 1.91
PD	85.68 \pm 1.87	84.33 \pm 2.03
PDD	102.47 \pm 4.66	95.33 \pm 4.64
Kruskal–Wallis ANOVA (p value)	<0.001	<0.001

The Kruskal–Wallis one way analysis of variance is showing significant difference for $T_{1\rho}$ across the cohorts

AD Alzheimer's disease, *PD* Parkinson's disease, *PDD* Parkinson's disease with dementia